Self-Assembly of Poly(ferrocenyldimethylsilane-*b*-methyl methacrylate) Block Copolymers in a Selective Solvent

Igor Korczagin,[†] Mark A. Hempenius,[†] Remco G. Fokkink,[‡] Martien A. Cohen Stuart,[‡] Mahmoud Al-Hussein,[§] Paul H. H. Bomans,[⊥] Peter M. Frederik,[⊥] and G. Julius Vancso*,[†]

MESA[+] Institute for Nanotechnology, University of Twente, 7500 AE Enschede, The Netherlands; Laboratory of Physical Chemistry and Colloid Science, Wageningen University, 6700 EK Wageningen, The Netherlands; FOM AMOLF Institute for Atomic and Molecular Physics, 1009 DB Amsterdam, The Netherlands; and Electron Microscopy-unit, Department of Pathology, Maastricht University, 6200 MD Maastricht, The Netherlands

Received November 25, 2005; Revised Manuscript Received January 23, 2006

ABSTRACT: The self-assembly of poly(ferrocenyldimethylsilane-*b*-methyl methacrylate) block copolymers, with PFDMS contents of 9−61 wt % (block ratios 1:23−1:1.5), is described. PFDMS-*b*-PMMA block copolymers form remarkable cylindrical micelles with very narrow diameter distributions at block ratios in the range of 1:10−1:6 (18−26 wt % PFDMS) in the block-selective solvent acetone, which is a good solvent for PMMA and a nonsolvent for PFDMS. The micelles, with a PFDMS core and a PMMA corona, were studied in solution by means of dynamic light scattering, ^{1}H NMR spectroscopy, and cryo-transmission electron microscopy. Micelles were also deposited on silicon substrates by dip-coating and characterized with atomic force microscopy and scanning electron microscopy. The micelles were over 3 μm long and had an overall diameter of around 22 nm. Dynamic light scattering experiments confirmed the formation of rodlike micellar aggregates in acetone. The cylindrical micelles exhibited a rod-to-sphere transition around 60 °C. When cooled below this transition temperature, the micelles reassembled back to their original aggregation state. Depolarized DLS experiments showed no rotational contribution to the measured decays of the autocorrelation functions. We ascribe this to the extreme length of the micelles, which arrests rotational movement. ^{1}H NMR spectra recorded in acetone-d_6 showed PFDMS signals, indicating that these blocks in the micellar cores have some mobility. This suggests that the cores are not in a crystalline state and that crystallization is not a driving force in the formation of these PFDMS-*b*-PMMA cylindrical micelles, but rather the contrast in solvophilicity between the blocks, which in the bulk are in the strong segregation limit.

Introduction

Recently we described the synthesis of a novel organic−organometallic block copolymer, poly(ferrocenylsilane-*b*-methyl methacrylate), using sequential anionic polymerization and atom transfer radical polymerization (ATRP).[1] By combining functional organometallic blocks with taylored organic blocks, new nanoscale, self-assembled systems for lithographic, catalytic, and other applications may be accessed.[2] Poly(ferrocenylsilane)s, PFS,[3] show a remarkable resistance toward dry etching with e.g. oxygen, CF_4, and SF_6 plasmas[4] and possess other potentially useful properties such as electrochemical[5] and catalytic[6] activity associated with the presence of iron atoms in the main chain. The self-assembly of hybrid organic−organometallic block copolymers in selective solvents is attracting much interest due to the variety of nanoscale structures that can be obtained and the potentially useful properties or functionality of the assemblies.[7] Cylindrical micelles obtained from PI-*b*-PFDMS and PFDMS-*b*-PDMS, for instance, were demonstrated to be efficient precursors for ceramic nanolines.[8,9] It has been proposed that crystallization of the core polymer (PFDMS) is the driving force for the formation of the cylindrical micelles.[10,11] Compared to the well-established polyisoprene,[12] polystyrene,[13] and poly(dimethylsiloxane)-based[9] PFDMS block copolymers, the poly(methyl methacrylate) (PMMA) block provides a higher contrast in polarity between the hydrophobic PFDMS and the organic block, enabling us to study the self-assembly of PFDMS-*b*-PMMA in polar block-selective solvents.

In most of the cases, regular asymmetric block copolymers self-assemble into spherical micelles when dissolved in a block-selective solvent. Literature accounts of asymmetric block copolymers forming cylindrical micelles in selective solvents are rather scarce. Examples of cylindrical aggregates include poly(styrene-*b*-isoprene) that forms long cylinders or lamellae in *N*,*N*-dimethylacetamide[14] or in decane.[15] A similar behavior was observed for poly(styrene-*b*-butadiene-*b*-styrene) in ethyl acetate where cylindrical micelles were formed at elevated temperatures.[16] This was explained in terms of a reversible polymerization process. Spherical micelles "polymerized" into long cylinders in order to reduce the core surface area per chain. Association into cylindrical micelles was also reported for poly(ethylene oxide-*b*-propylene oxide-*b*-ethylene oxide) in water.[17] Other examples of cylindrical aggregates include copolymers with polystyrene as one block and a polar second block such as poly(acrylic acid),[18] poly(2-vinylpyridine),[19] poly(ethylene oxide),[20] or poly(2-cinnamoylethyl methacrylate)[21] and poly(methyl methacrylate-*b*-perfluorooctyl methacrylate).[22]

Block copolymer molar mass, volume or mass fraction, and chemical composition of the constituent blocks determine the morphologies obtained by block copolymer self-assembly in bulk. In selective solvents, the structure of block copolymer

[†] University of Twente.
[‡] Wageningen University.
[§] FOM AMOLF Institute for Atomic and Molecular Physics.
[⊥] Maastricht University.
* Corresponding author: Ph +31 53 4892974; Fax +31 53 4893823; e-mail g.j.vancso@utwente.nl.

10.1021/ma052521i CCC: $33.50
Published on Web 02/18/2006

Table 1. Molecular Characteristics of the PFDMS-*b*-PMMA Block Copolymers

	PFDMS block	PFDMS-*b*-PMMA			
polymer	M_n[a] (g/mol)	M_n[a] (g/mol)	M_w/M_n	PFDMS content[b] (wt %/vol %)	bulk morphology[c]
1 $PFDMS_{50}$-*b*-$PMMA_{1162}$	12 000	101 700	1.10	0.09/0.08	BCC
2 $PFDMS_{50}$-*b*-$PMMA_{531}$	12 000	66 900	1.06	0.18/0.17	BCC
3 $PFDMS_{50}$-*b*-$PMMA_{341}$	12 000	40 500	1.18	0.26/0.24	HEX
4 $PFDMS_{92}$-*b*-$PMMA_{140}$	22 000	79 700	1.32	0.61/0.59	LAM

[a] Determined by size exclusion chromatography, based on polystyrene standards. M_w/M_n of the PFDMS block = 1.05. [b] Weight percent of PFDMS block calculated from ^{1}H NMR integrals. Volume percentage calculated taking densities of PFDMS and PMMA to be 1.26 and 1.15 g/cm^3, respectively. [c] Estimated using the phase diagram constructed by Rehahn et al.[25] and SAXS measurements.

Scheme 1. Chemical Structure of the PFDMS-*b*-PMMA Block Copolymers

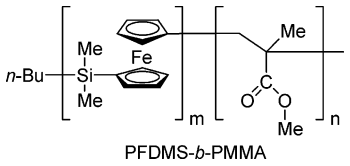

PFDMS-*b*-PMMA

micelles is controlled by these parameters and by the selectivity of the solvent for the different blocks: the insoluble block tends to minimize contact with the solvent (which favors large aggregates), but the soluble block tends to swell in the solvent, forming a corona. In a dense corona, the chains repel each other by osmotic forces, and they will stretch, at the expense of some entropy, to lower the osmotic energy. The balance between core solvophobicity and corona osmotic pressure determines the local curvature. If the curvature is very high, spherical micelles are always favored, whereas other structures (cylinders or sheets) can appear at lower curvatures.[23] In this contribution, the self-assembly and characterization of PFDMS-*b*-PMMA block copolymers with varying block ratios in acetone are described.[24]

Experimental Section

Materials. Tetrahydrofuran (THF, ≥99.0%) and acetone (≥99.5%) were obtained from Aldrich. All solvents were filtered through 200 nm pore size filters (Schleicher & Schuell Spartan 13/0,2 RC) to remove dust particles. Poly(ferrocenyldimethylsilane-*b*-methyl methacrylate) block copolymers were synthesized as described earlier.[1] Molecular characteristics of the investigated block copolymers are given in Table 1.

Preparation of Micellar Solutions. Block copolymers were first dissolved in THF, a good solvent for both blocks, followed by the dropwise addition of a block-selective solvent (acetone). The resulting solutions always contained 10 vol % of THF.

Deposition of Micelles. Micelles were deposited on cleaned silicon wafers [100] with a native oxide layer by dip-coating from 10 mg/mL block copolymer solutions in acetone (selective solvent) or chloroform (nonselective solvent). A custom-built dip-coater with a stepper motor was used. The substrates were withdrawn with speeds ranging from 100 μm/s to 1 mm/s.

Characterization Techniques. Deposited micelles were investigated by atomic force microscopy (Digital Instruments NanoScope IIIa). Standard Si_3N_4 tips (Pointprobe, Nanosensors) were used. The images were acquired in ambient air using the tapping mode. Micelles were studied with an amplitude of oscillation at free vibration of $A_0 = 2.0$ V and with operating set point ratios having a value of $A/A_0 = 0.6-0.9$. Scanning electron microscopy images were captured by a LEO Gemini 1550 FEG-SEM setup. ^{1}H NMR spectra were recorded in $CDCl_3$ and acetone-d_6 using a Varian Unity 400 spectrometer at 399.9 MHz. Dynamic light scattering experiments were performed using an ALV light scattering instrument equipped with a 400 mW argon ion laser tuned to a wavelength of 514 nm. Temperatures were controlled by a Haake C35 thermostat, providing an accuracy of ±0.1 K. To analyze the measured autocorrelation functions, the method of cumulants[26] was used (DynaLS software from Alango Ltd.). Depolarized dynamic light scattering was performed in order to determine the rotational diffusion coefficient. For measurements in the depolarized configuration (VH, vertical horizontal), the polarization filter was set at 90° with respect to the laser light polarization (all the light in the polarization plane of the laser was blocked). In the polarized configuration (VV, vertical vertical), the filter was set at 0° relative to the polarization of the light source. Samples for cryo-TEM measurements were made by placing a small droplet (3 μL) of polymer solution (1 mg/mL, 90% acetone and 10% THF) on a Quantifoil R2/2 grid precleaned with acetone to remove soluble debris. Excess liquid was blotted away, and the thin specimen thus formed was plunged into the cryogen, liquid nitrogen, using a vitrification robot (Vitrobot, FEI Co., Hillsboro, OR) with a specimen chamber saturated with acetone vapor.[27] The grids with vitrified thin films were analyzed in a CM-12 transmission microscope (Philips, Eindhoven, The Netherlands) at −172 °C using a Gatan-626 cryo-specimen holder and cryo-transfer system (Gatan, Warrendale, PA). The vitrified films were studied at 120 kV at a pressure lower than 0.2×10^{-3} Pa, and at standard low-dose conditions, micrographs were taken. Small- and wide-angle X-ray scattering (SAXS and WAXS) measurements were conducted using an in-house setup with a rotating anode X-ray generator (Rigaku RU-H300) operating at 18 kW. By employing two parabolic multilayer mirrors (Bruker, Karlsruhe), a highly parallel beam of a monochromatic Cu Kα radiation ($\lambda = 0.154$ nm) with a divergence of 0.012° was obtained. The SAXS patterns were recorded with a Bruker Hi-Star area detector at a sample-to-detector distance of 1.03 m. The two-dimensional scattering patterns were radially integrated, corrected for the background, and then displayed as one-dimensional plots of the intensity as a function of q, the magnitude of the scattering vector. The WAXS curves were recorded using a linear position sensitive detector (PSD-50M, Braun).

Results and Discussion

Dynamic Light Scattering. Dynamic light scattering was used to investigate the morphology of PFDMS-*b*-PMMA micelles directly in solution. First, the influence of solvent quality was investigated by recording the formation of micelles upon the gradual addition of a PMMA-selective solvent (acetone, nonsolvent for PFDMS) to the nonselective solvent THF. Several solutions of the same concentration (1 mg/mL) were prepared by dissolving the block copolymers in mixtures of acetone and THF. Autocorrelation functions of scattered light intensity were recorded for each solution, and an average scattered light intensity was used as a measure of the extent of micelle formation. To take into account changes in solvent refractive index, the translational diffusion coefficients were calculated using the method of cumulants.[26] The results are shown in Figure 1 and Figure 2.

It can be clearly seen in Figure 1 that polymers with a low PFDMS content (**1**, **2**, and **3**) show a substantial increase in scattered light intensity only when acetone makes up more than 70% of the solvent. In the case of the polymer with a majority PFDMS phase (**4**), the scattered light intensity begins to increase already at 50% of acetone. Similar trends were observed in the solvent composition dependence of diffusion coefficients (Figure

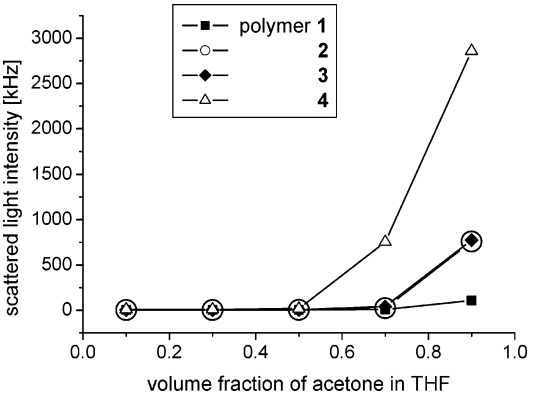

Figure 1. Influence of acetone content on PFDMS-*b*-PMMA micelle formation. Polymers **1**−**4** have PFDMS/PMMA block ratios of 1:23, 1:10, 1:6, and 1:1.5, respectively (see Table 1). Polymer concentration 1 mg/mL. Scattered light intensity was measured at an angle of 90°.

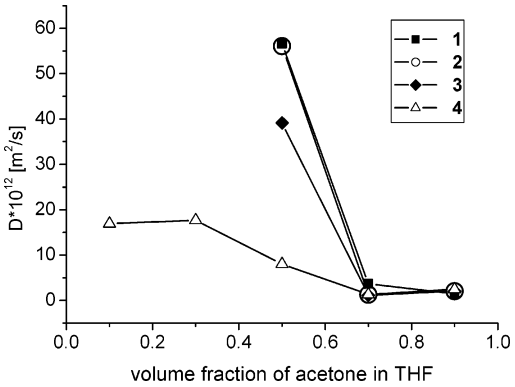

Figure 2. Translational diffusion coefficient as a function of acetone content. Polymers **1**−**4** have PFDMS/PMMA block ratios of 1:23, 1:10, 1:6, and 1:1.5, respectively (see Table 1).

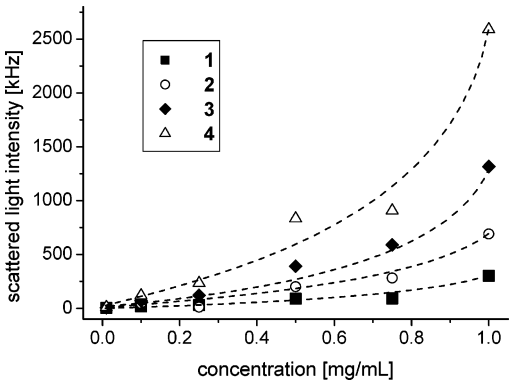

Figure 3. Concentration dependence of the scattered light intensity of micellar solutions in acetone with 10 vol % THF. Polymers **1**−**4** have PFDMS/PMMA block ratios of 1:23, 1:10, 1:6, and 1:1.5, respectively (see Table 1). The dashed lines are shown to indicate trends.

2). For polymers with a minority PFDMS content in solvent mixtures with less than 50% acetone, no meaningful diffusion coefficients could be obtained due to very weak scattering (i.e., no micelles were formed). At acetone contents above 70% the values of the diffusion coefficients level off, indicating the formation of fully developed micelles. Polymer **4** with a PFDMS majority forms aggregates that scatter light at much lower acetone contents. The diffusion coefficient begins to drop at about 40% of acetone in solution and levels off at 70%.

The concentration at which the micelles are first formed is known as the critical micelle concentration (cmc). Figure 3 shows the concentration dependence of the scattered light intensity for PFDMS-*b*-PMMA micelles in acetone (with 10

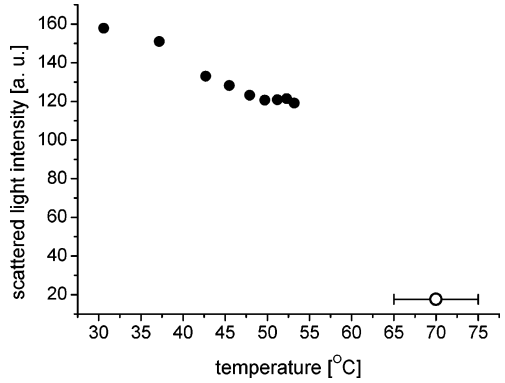

Figure 4. Decrease in scattered light intensity upon heating of a 1 mg/mL solution of PFDMS-*b*-PMMA micelles (**3**, block ratio 1:6**)** in acetone.

vol % THF). At a concentration of 10^{-2} mg/mL autocorrelation functions could still be recorded; i.e., we could not establish a cmc for these systems. The aggregation behavior of PFDMS-*b*-PMMA in acetone changes at high temperature. At temperatures close to the boiling point of acetone (56.2 °C), the opalescent micellar solution became transparent. This indicates that either existing micelles transformed into other, smaller micelles or into individual block copolymer molecules, dissolved in acetone as unimer micelles. Figure 4 illustrates the decrease in scattered light intensity upon increasing the solution temperature. The point indicated as an open circle (○) corresponds to a measurement performed immediately after heating a solution of polymer **3** (1 mg/mL) in a tightly closed cuvette to ∼65−70 °C. The translational diffusion coefficient measured immediately after the block copolymer solution became transparent corresponded to spherical micelles with a diffusion radius of 34 nm, calculated using the Stokes−Einstein equation. This implies that at a transition temperature around 60 °C larger micellar aggregates transform into smaller spherical micelles. The scattered light intensity was further measured as a function of temperature (Figure 4). Manners et al. obtained spherical micelles when heating PFDMS-*b*-PDMS cylindrical micelles in *n*-decane to 150 °C, quenching in ice, and leaving the solutions at room temperature. The rod-to-sphere transition in that case took place at higher temperatures and was ascribed to the melting of the crystalline PFDMS micellar core.[10] These authors concluded that when micelles were formed below the bulk T_m of PFDMS (120−145 °C), cylindrical micelles result. Above T_m, spherical micelles are formed.

To investigate the kinetics of micelle formation, we followed the changes in scattered light intensity in time after overheating the block copolymer solution in acetone above the mentioned transition temperature to an estimated 65 °C and subsequently "quenching" the system to 55 °C. Changes in scattered light intensity and in translational diffusion coefficient are shown in Figure 5. The time dependence of the scattered light intensity has a sigmoidal shape. It shows early exponential growth of scattering intensity, which slows to linear growth after ∼1000 s, and then approaches intensities corresponding to fully developed cylindrical micelles. At the same time the diffusion coefficient decreases and levels off after about 2400 s at values observed for cylindrical micelles prior to heating. At room temperature, cylindrical micelles are formed even faster.

Figure 6 shows autocorrelation functions of the scattered light intensity of PFDMS-*b*-PMMA micelles in acetone. Solid lines represent single-exponential decay fits to data points recorded immediately after overheating the solution (curve A) to ∼65 °C and after a recovery time (curve B) necessary for the

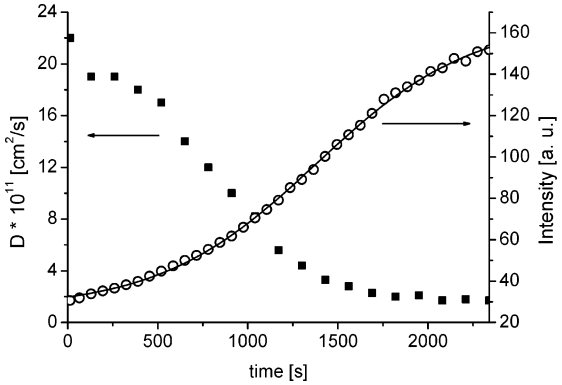

Figure 5. Formation of PFDMS-*b*-PMMA micelles (**3**, block ratio 1:6) upon "quenching" from above the rod-to-sphere transition temperature to 55 °C in acetone. Intensity of the scattered light (○); the line represents a sigmoidal fit to the data. Translational diffusion coefficient (■).

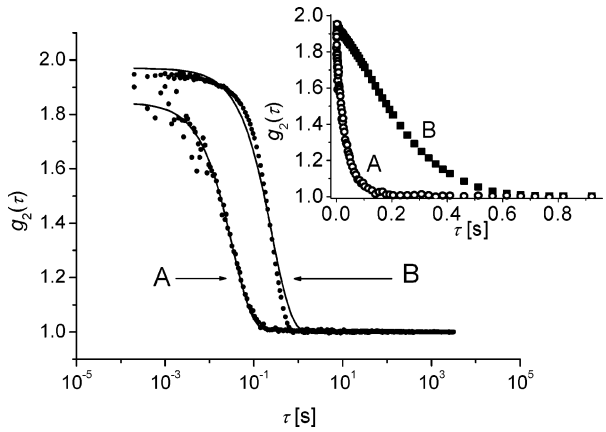

Figure 6. Autocorrelation function of PFDMS-*b*-PMMA micelles (**3**, block ratio 1:6) in acetone (1 mg/mL) formed immediately after overheating (A) and fully developed cylindrical micelles at 55 °C (B). Solid lines represent single-exponential decay fits to the data (R^2 was 0.993 and 0.996 for A and B, respectively). The inlay shows a lin−lin plot of the autocorrelation functions recorded at 90° scattering angle.

formation of fully grown cylindrical micelles as observed prior to heating. The autocorrelation function of the heated solution (A) fits very well to the single-exponential model with a decay constant Γ_A on the order of 17 Hz, which corresponds to a spherical micelle with a radius of 34 nm. The fit to curve B gives a much lower average decay rate of $\Gamma_B = 1.7$ Hz, consistent with micelles diffusing roughly 10 times more slowly. The fit to curve B is evidently less good compared to curve A, which is consistent with the different geometry and polydispersity of the cylindrical micelles.

Temperature-Dependent ^{1}H NMR Studies in Acetone. The DLS measurements were complemented with high-temperature ^{1}H NMR measurements of PFDMS-*b*-PMMA (**3**, block ratio 1:6) in deuterated acetone. Usually the mobility of protons inside of micellar cores is hindered to such an extent that the width of the corresponding NMR lines can broaden on the order of hundreds of hertz or more, so that these protons escape detection in high-resolution spectra. NMR studies focused on micelles with a polystyrene core showed that at room temperature polystyrene peaks were absent from spectra, indicating that the PS core was glassy.[28] As the temperature was increased, the PS peaks gradually appeared in the spectrum as the core chains became more mobile. The core peaks were fully developed before the critical micelle temperature was reached. In *n*-octane such a "glass" transition of the core takes place some 50 °C lower than the bulk PS glass transition, presumably owing to plasticization by absorbed solvent molecules.[29] Figure 7 presents the ^{1}H NMR spectra of a PFDMS-*b*-PMMA block copolymer recorded in deuterated acetone and in deuterated chloroform. In acetone at 25 °C the PFDMS signal is still visible, indicating that the micellar cores (containing the PFDMS block) are mobile, which may be explained by some degree of plasticization by solvent molecules. The presence of the PFDMS signals in the ^{1}H NMR spectrum strongly suggests that in the micellar solution the PFDMS block is not in a crystalline state. The absence of polymer crystals in the micellar core was further confirmed by X-ray scattering experiments. WAXS measurements performed on deposited micellar films showed no Bragg peaks, which indicates that the PFDMS domains of our block copolymers are not crystalline. Therefore, we believe that the principal driving force for the micellar self-assembly of PFDMS-*b*-PMMA is the difference in solvophilicity of the hydrophobic PFDMS and the relatively polar PMMA block. In the bulk, PFDMS-*b*-PMMA is regarded as strongly phase segregating[25] while e.g. PS-*b*-PFDMS is in the weak segregation limit.[30]

Dynamic Depolarized Light Scattering. Depolarized light scattering experiments can be a source of structural information not readily obtainable by other techniques. This technique is especially useful when applied to dilute solutions of rigid particles or molecules with optical anisotropy.[31] The most common model assumes that such species undergo independent rotational and translational diffusion. It has also been shown that the correlation function of such rodlike or ellipsoidal molecules or particles measured in the depolarized configuration (VH) exhibiting a monomodal sharp size distribution consists of one decaying exponential ($\Gamma = q^2D + 6\Theta$, where D and Θ are translational and rotational diffusion coefficients, respectively).[32]

Figure 8 shows the angular dependence of the decay constant of the autocorrelation functions for depolarized dynamic light scattering experiments performed in acetone solutions of polymers **2** and **3**. For comparison, results obtained in conventional polarized DLS are also plotted. The values of Γ were calculated using the method of cumulants.[26,33] The analysis of the cumulant expansion of the correlation function was performed by fitting third-order polynomials to the function $\ln[g_{(2)}(\tau) - 1]$.[33] The value of the translational diffusion constant observed was on the order of 10^{-15} m^2 s^{-1} ($D_3 = (2.2 \pm 0.6) \times 10^{-15}$ m^2 s^{-1} and $D_2 = (2.6 \pm 0.4) \times 10^{-15}$ m^2 s^{-1}). If we assume a cylindrical morphology, the observations would correspond to a cylinder length of over 3 μm (calculated using Broersma's expressions[34] and assuming a diameter of 18.5 nm based on SEM images).[35] For comparison, the tobacco mosaic virus, which has a similar diameter and a length of 300 nm, has a translational diffusion coefficient on the order of 3.6×10^{-12} m^2 s^{-1} and a corresponding rotational diffusion coefficient of 300 s^{-1}.[17c] Somewhat longer cholesterol micelles ($L = 580$ nm) rotate 3 times slower ($\Theta = 110$ s^{-1} and $D = 4.3 \times 10^{-12}$ m^2 s^{-1}).[32b]

It is difficult (if at all possible) to estimate the value of the rotational coefficient for our system. The values of decay constants extrapolated to zero scattering vector tend to approach or oscillate around zero with large error values. This indicates that there is little or no rotational contribution, probably because the micelles are too long to reorient on time scales associated with translation. The normalized autocorrelation functions recorded in polarized (VV) and depolarized (VH) configurations, shown in Figure 9, can be fitted with single-exponential decay functions with similar decay constants. This again shows that the contribution of rotational diffusion to the scattered light

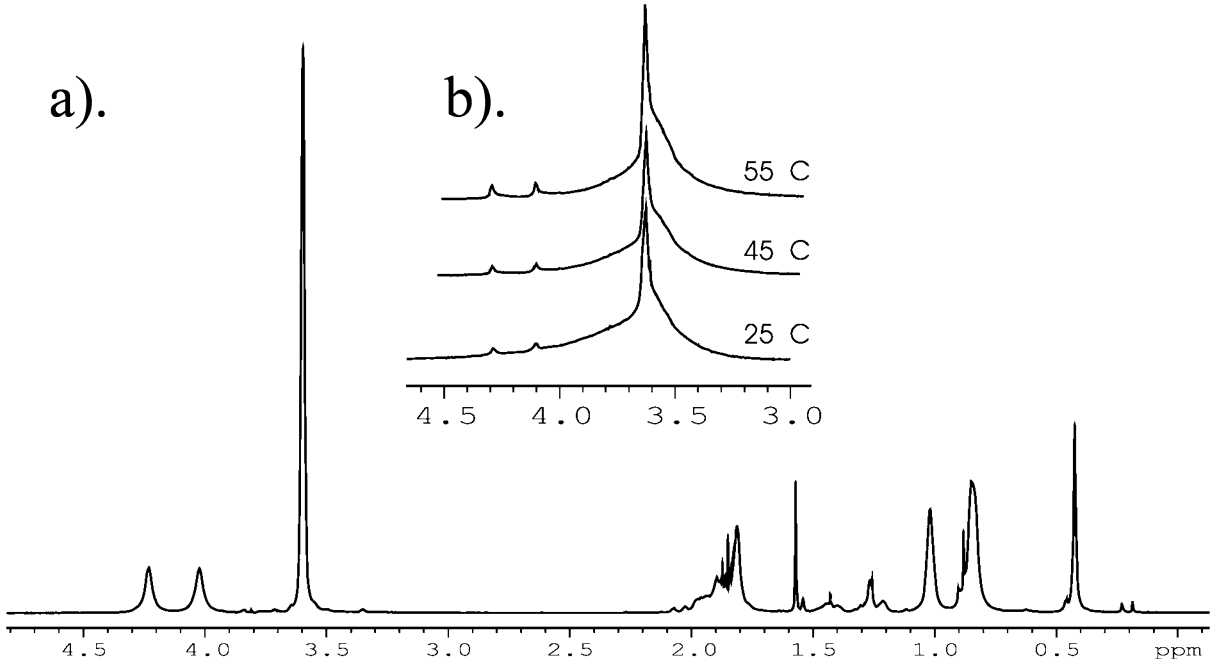

Figure 7. 400 MHz ^{1}H NMR spectra of PFDMS-*b*-PMMA (**3**, block ratio 1:6). (a) Spectrum recorded in $CDCl_3$ (a good solvent for both blocks) at 25 °C. (b) Spectra recorded in acetone-d_6 at different temperatures. Characteristic ferrocene signals of the PFDMS block are at $\delta = 4.01$ and 4.22 ppm. The methoxy ($-OCH_3$) signal of the PMMA block is at $\delta = 3.60$ ppm.

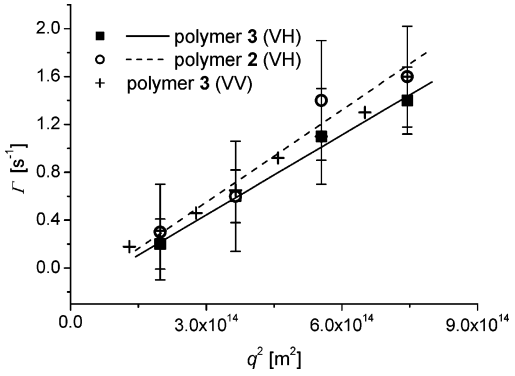

Figure 8. Depolarized dynamic light scattering (VH) angular dependence of measured decay constants. Polymer concentration 1 mg/mL in acetone (with 10 vol % THF). Solid and dashed lines represent linear fits to decay constants as a function of q of solutions of polymers **2** and **3** (PFDMS/PMMA block ratios 1:10 and 1:6, respectively). For comparison, results obtained from polarized light scattering (VV) are also plotted for polymer **3** in acetone (+).

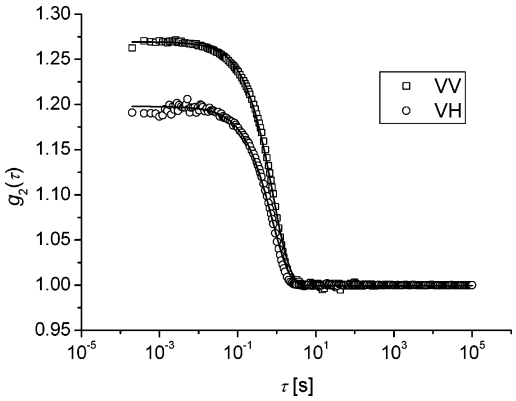

Figure 9. Normalized autocorrelation functions of polarized (□) and depolarized (○) measurements. Polymer **3** solution in acetone at a scattering angle of 70°. The lines represent a single-exponential fit to the measurement points.

signal is very small. These two autocorrelation functions differ only in the intensity of the signal. Scattered light recorded in the VH configuration had a much lower intensity, on the order of 1% of the polarized scattered light intensity. Moreover, just as in the case of PFDMS-*b*-PDMS cylinders,[9] we also observed no second relaxation mode in polarized DLS, which would be characteristic of rodlike structures. This can be due to the flexibility of the cylinders and also due to their extreme length ($L/d > 170$).

In summary, the DLS experiments give further indication in support of the formation of long micellar aggregates in acetone. The micelles exhibit a critical micelle temperature, above which they transform into spherical micelles. When quenched below the cmt, the micelles reassemble back to their original aggregation state. Depolarized DLS experiments show no rotational contribution to the measured decays of the autocorrelation functions. We ascribe this to the extreme length of the micelles, which arrests rotational movement.

Cryogenic Transmission Electron Microscopy. The DLS results were confirmed by performing cryo-TEM measurements on micellar solutions of block copolymers in the same solvent mixture (90 vol % acetone and 10 vol % THF), using the same polymer concentration (1 mg/mL). By performing transmission electron microscopy measurements on frozen block copolymer solutions, influences of substrates and drying of the aggregates do not play a role, thus ensuring that the obtained images faithfully represent the aggregation of the polymer chains in a block-selective solvent. The cryo-TEM micrographs of acetone solutions of polymers **2** and **3** (shown in Figures 10 and 11) confirm the results obtained in the DLS experiments. The polymers indeed aggregate into anisotropic wormlike micelles of an extreme length, with an overall diameter of 28 nm in the case of polymer **2** and 22 nm for polymer **3**.

Surface Deposition of Micelles. In further studies we wanted to investigate whether the micelles formed in a selective solvent could be used in the surface decoration of silicon substrates in view of their potential use in reactive ion etching-assisted lithography.[8] Micelles were deposited on silicon substrates by dip-coating. The coating process was carried out by slowly

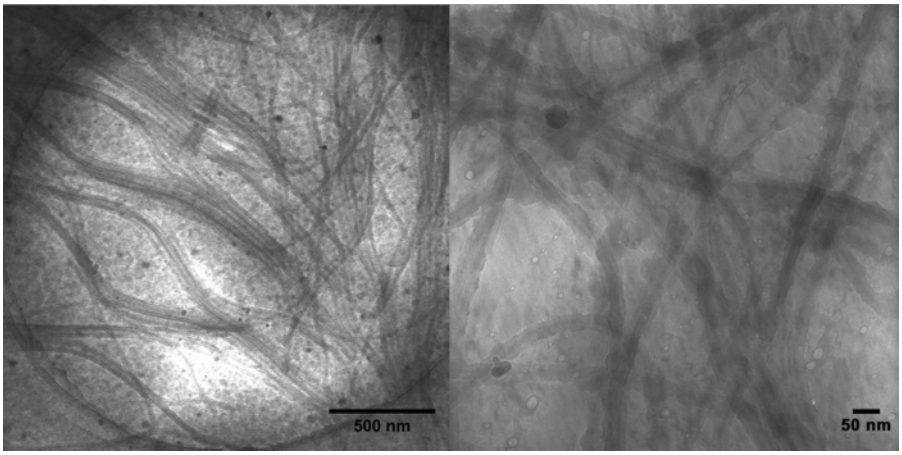

Figure 10. Cryo-TEM micrographs of a 1 mg/mL solution of polymer **2** (PFDMS/PMMA block ratio 1:10) in acetone.

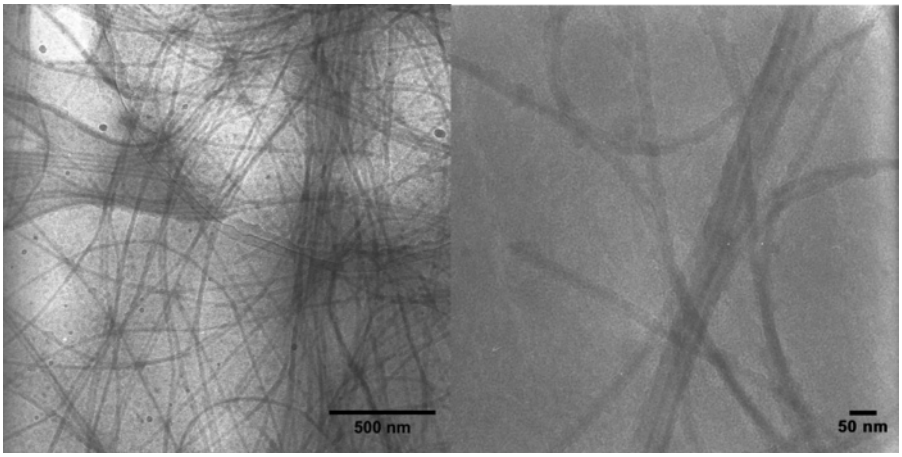

Figure 11. Cryo-TEM micrographs of a 1 mg/mL solution of polymer **3** (PFDMS/PMMA block ratio 1:6) in acetone.

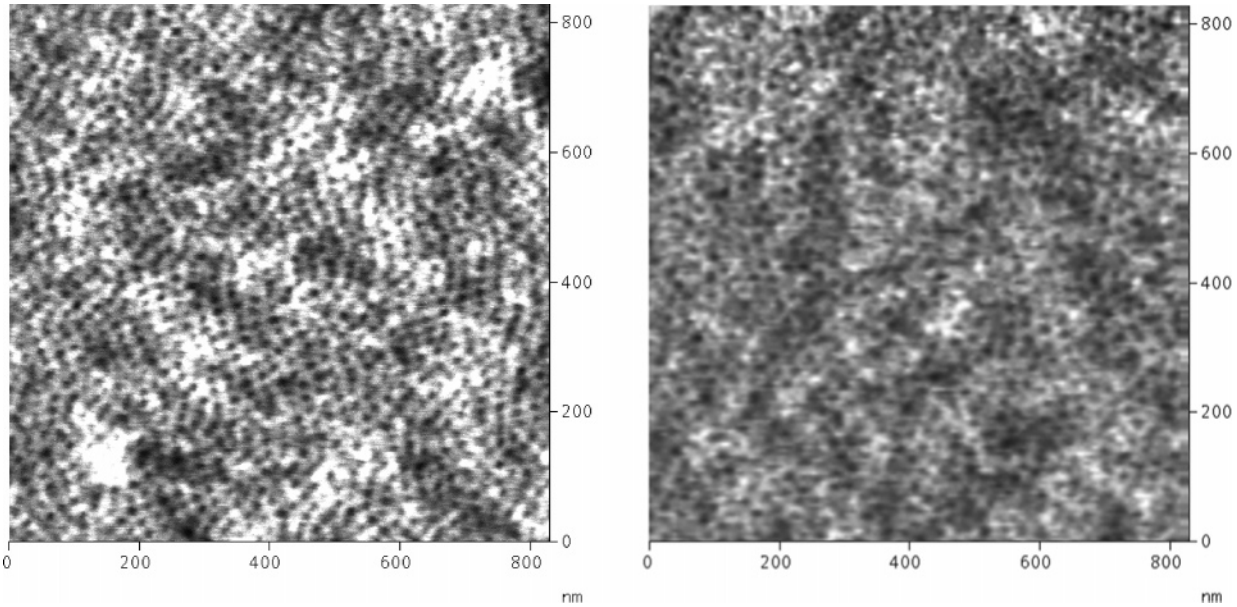

Figure 12. AFM height images of polymer **2** (left) and **3** (right) films prepared by dip-coating of silicon substrates using nonselective solvent solutions (7 mg/mL of chloroform). The withdrawing speed was 250 μm/s. The *z*-scale is 5 nm.

withdrawing Si slides from block copolymer micellar solutions. After deposition, the substrates were imaged with tapping mode AFM. This allowed us to investigate the influence of the block copolymer composition on micellar morphology. Samples dip-coated in a chloroform solution (good solvent for both blocks) always resulted in patterns exhibiting typical circular motifs characteristic of phase-separated block copolymer films with a spherical morphology, even though for some blocks this was not the equilibrium bulk morphology (see Figure 12). Upon withdrawal of a substrate, a meniscus is formed due to capillary rise. In this meniscus solvent evaporation takes place, and a thin film of block copolymer is deposited. Slowly evaporating

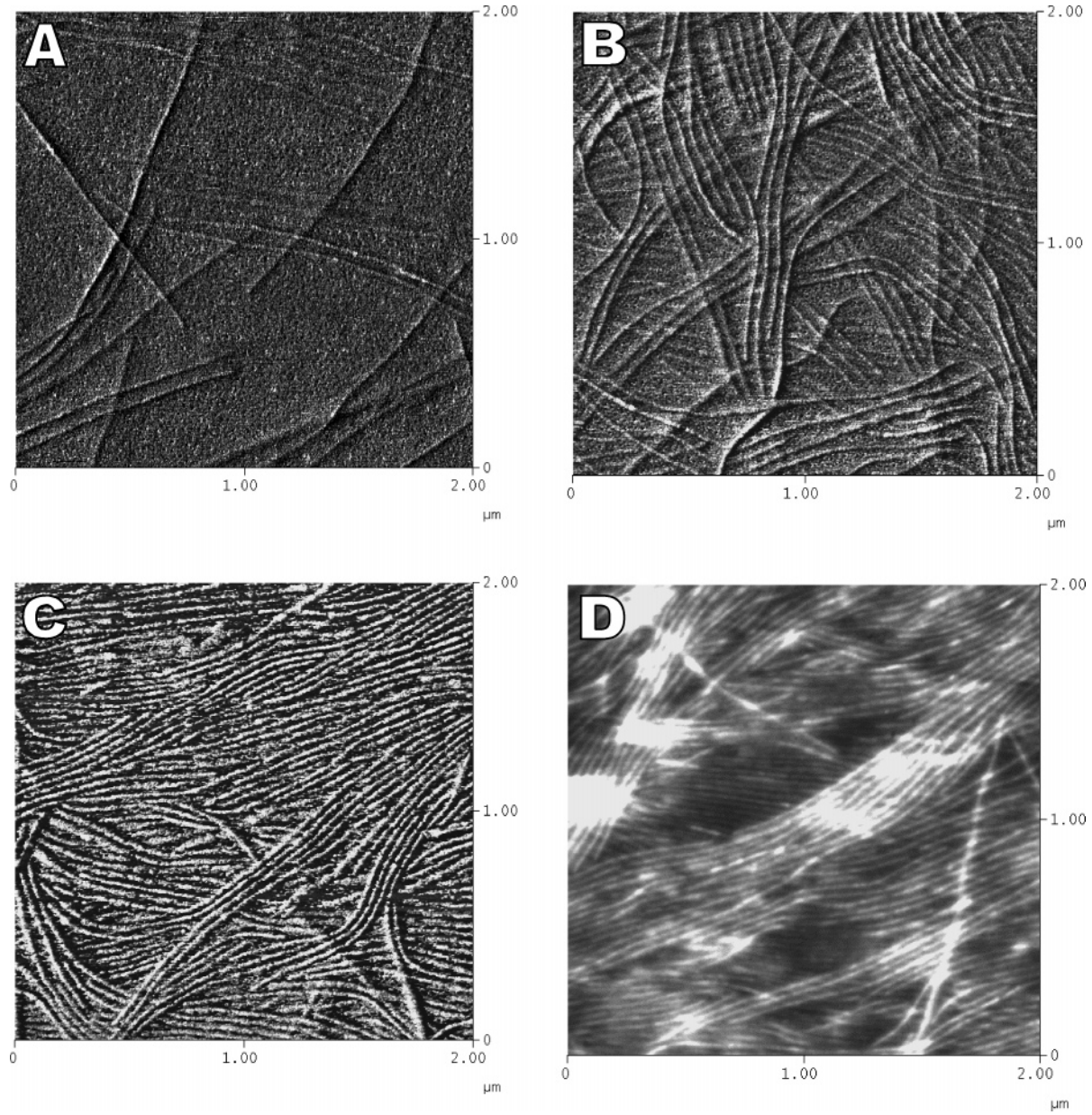

Figure 13. AFM phase images of silicon substrates dip-coated in a solution of PFDMS-*b*-PMMA in acetone. Polymers: (A) **1**, (B) **2**, (C) **3**. Phase contrast 30°−50°. (D) AFM height image of a polymer **3** sample (*z*-scale 15 nm).

solvent provides enough mobility for the block copolymer chains, and microphase separation takes place during the withdrawing process. This simultaneous film deposition and ordering is a result of the interplay between solvent evaporation rate, solvent partial vapor pressure, and withdrawing speed. In practice, it can be regarded as zone solvent annealing.[36]

The interdomain spacing of the circular motifs obtained by dip-coating from chloroform (20−23 nm) corresponds quite well to the block copolymer bulk values. SAXS measurements performed on the bulk copolymer samples revealed an interdomain period of 25 nm in the case of polymers **2** and **3** and 40 nm for polymer **4**. Their corresponding phase morphology was further established using the SAXS data and the phase diagram constructed by Kloninger and Rehahn (see also Table 1).[25] A different picture appears when substrates are dipped into a solution of block copolymer already preorganized in a selective solvent. Figure 13 shows AFM images of deposited micelles made of polymers with different PFDMS contents.

Dip-coating from acetone solution resulted in deposition of cylindrical micelles. However, substrates covered with block copolymer **1**, containing 9 wt % of PFDMS (PFDMS/PMMA block ratio 1:23), showed a limited number of cylindrical micelles which were partially embedded in a phase-separated block copolymer film with a spherical domain morphology as evidenced by AFM height images. This morphology can be seen even more clearly after annealing of the samples at 160 °C, which is above the equilibrium melting temperature of poly(ferrocenyldimethylsilane) in bulk.[37] Remarkably, the cylinders seem to remain intact and retain their initial size and shape following annealing (see Figure 14).

The existence of the two morphologies indicates that while some material had associated into cylinders, most of PFDMS-*b*-PMMA block copolymer **1** was present as spherical micelles in acetone. This is also consistent with the DLS measurements, where block copolymer **1** exhibited the lowest scattered light intensity in the whole series. An increase in the block copolymer

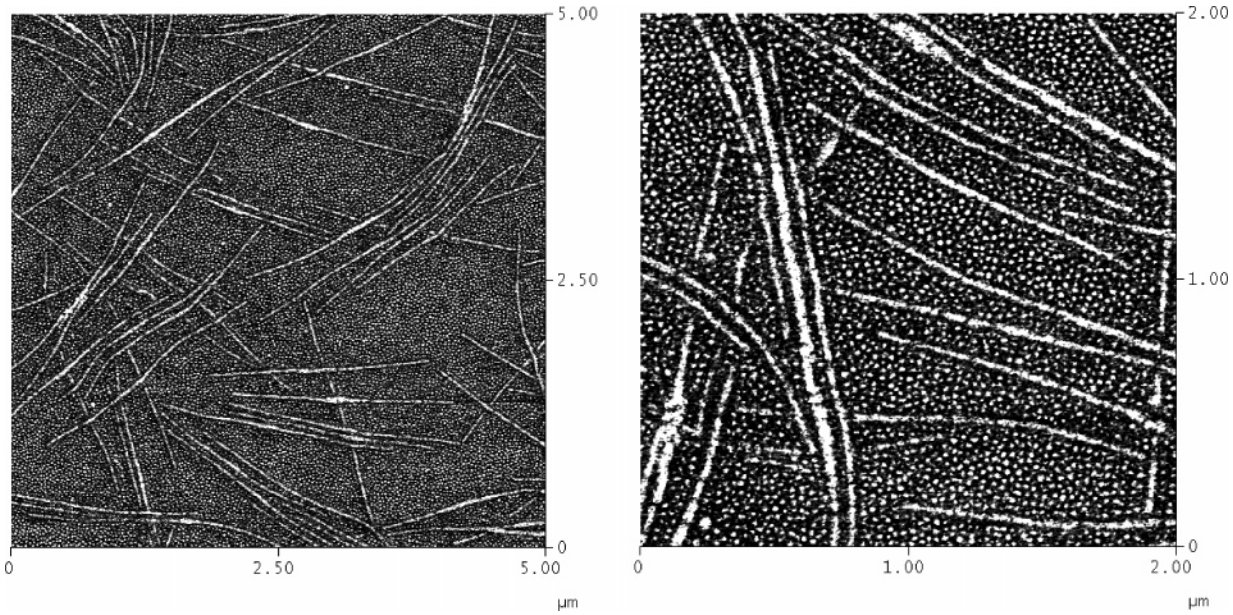

Figure 14. AFM phase images of a block copolymer **1** sample (PFDMS/PMMA block ratio 1:23, the same sample as shown in Figure 13A) after annealing in a vacuum at 160 °C for 24 h. Phase scale is 10°.

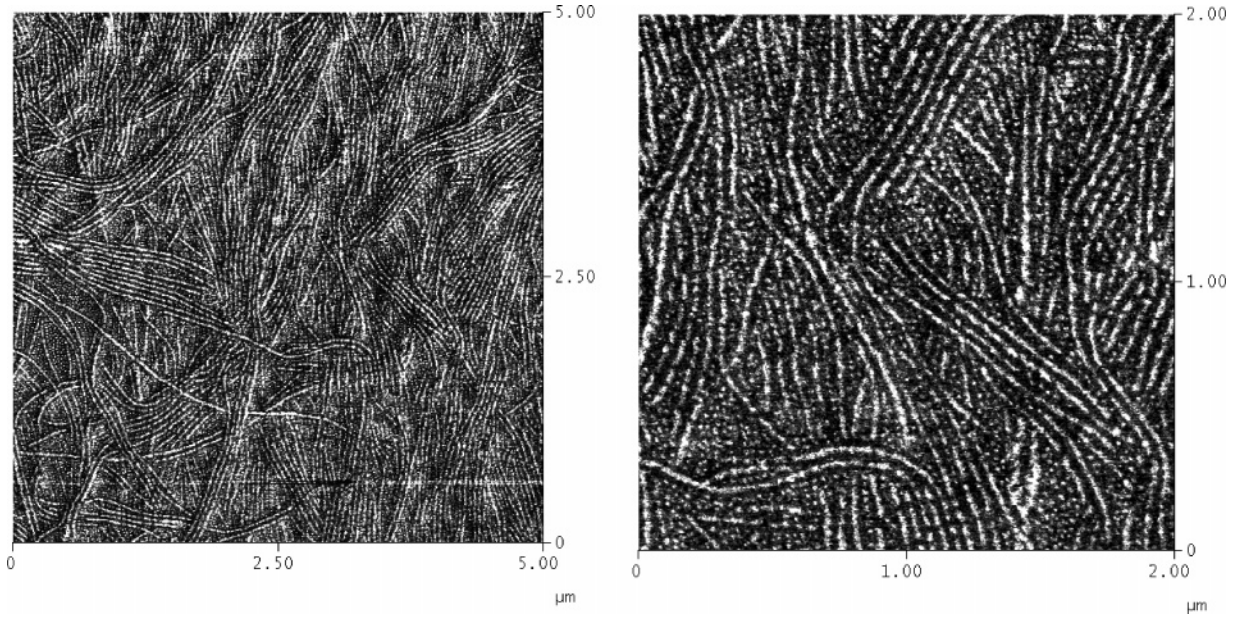

Figure 15. AFM phase images of a polymer **2** sample (PFDMS/PMMA block ratio 1:10, the same sample as shown in Figure 13B) after annealing in a vacuum at 160 °C for 24 h. Phase scale is 5°.

PFDMS content from 9 to 18 wt % was reflected in a higher scattered light intensity, suggesting that more cylinders are being formed. This in turn should result in an increase in the areal density of cylinders in the film as compared to the previous polymer. A dipped film prepared from polymer **2** containing 18 wt % of PFDMS (PFDMS/PMMA block ratio 1:10) was composed almost entirely of long cylindrical micelles. In some places the region between the cylinders showed a microphase-separated morphology similar to the previous example. Similar to the case of polymer **1**, annealing of the films accentuated this coexistence of two types of morphologies (see Figure 15).

Finally, films prepared from micellar solutions of polymer **3**, containing 26 wt % of PFDMS (Figure 13C), were entirely composed of long micelles with a diameter of 18 nm (17.9 ± 0.4 nm, estimated from AFM measurements). Figure 16 shows the SEM micrograph of polymer **3** micelles confirming the AFM results: the cylinders are 18.5 ± 0.3 nm in diameter and possess a length of at least 3 μm. The extreme length of these cylinders induced some local orientational ordering of the micelles confined in a 2D film.

The block copolymer with a majority PFDMS content, **4**, does not form cylinders (data not shown). Instead, spherical aggregates with diameters ranging from 20 to 200 nm were observed. The absence of cylindrical micelles can be easily explained by the fact that there is simply too much PFDMS and not enough PMMA to facilitate formation of such micelles. In this case one could expect the formation of large crew-cut micelles.[23b] Much higher scattered light intensity of polymer **4** solutions in acetone suggests that indeed larger aggregates are being formed in solution. This was confirmed by cryo-TEM

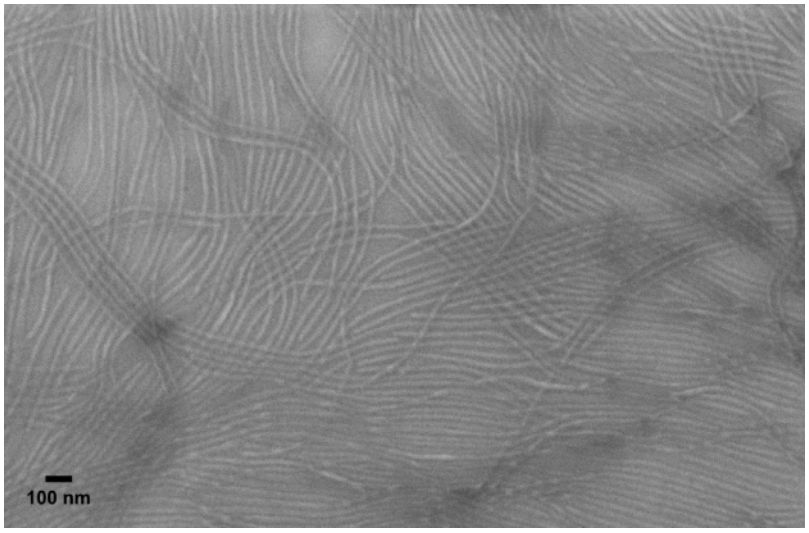

Figure 16. SEM image of block copolymer **3** micelles (PFDMS/PMMA block ratio 1:6) deposited on a silicon substrate from acetone solution.

measurements. Clearly, cylindrical micelles are formed only by block copolymers with an appropriate PFDMS content, at block ratios in the range of 1:10−1:6 (polymers **2** and **3**).

Conclusions

PFDMS-*b*-PMMA block copolymers self-assemble into micelles in the PMMA-selective solvent acetone. The micellar morphology depended on the length of the PFDMS block with respect to the PMMA block. The block copolymer with the lowest PFDMS/PMMA block ratio, 1:23, formed monomolecular or small spherical micelles with only a small fraction of polymer associating into cylindrical micelles. As the PFDMS fraction increased, a larger proportion of copolymer chains aggregated into cylindrical micelles. Cryo-TEM measurements in frozen acetone showed that long, cylindrical micelles were formed by PFDMS-*b*-PMMA block copolymers at PFDMS/PMMA block ratios of 1:10−1:6. At a block ratio of 1:6, the block copolymers formed well-defined cylindrical micelles exclusively, with an overall diameter of 22 nm and a length of over 3 μm. When PFDMS was in the majority, only crew-cut spherical aggregates were formed. Dynamic light scattering experiments provided evidence in support of the formation of long cylindrical micelles. The micellar solutions exhibited a rod-to-sphere transition temperature around 60 °C. At this temperature, cylindrical micelles transformed into spherical micelles with a hydrodynamic radius of 34 nm as calculated using the Stokes−Einstein equation.

High-resolution ^{1}H NMR studies of the micellar solutions in acetone-d_6 recorded at temperatures varying from 25 to 55 °C showed that the PFDMS core is in a mobile state, and solvent molecules penetrate inside of the micellar core. We therefore believe that the contrast in polarity between the two blocks, supported by the polar block-selective solvent, rather than crystallization of the PFDMS block, is the primary driving force of PFDMS-*b*-PMMA micelle formation. Cylindrical micelles with coronas composed of relatively high-T_g polymers such as PMMA constitute an excellent choice for surface deposition as precursors to ceramic nanolines due to the high stability of the cylinders.

Acknowledgment. The authors acknowledge the MESA$^+$ Institute for Nanotechnology and the European Community's Human Potential Programme under Contract HPRN-CT1999-00151, PolyNano, for financial support. Dr. Francesca Corbellini is gratefully acknowledged for performing the NMR experiments.

References and Notes

(1) Korczagin, I.; Hempenius, M. A.; Vancso, G. J. *Macromolecules* **2004**, *37*, 1686.
(2) For general references on block copolymers see: (a) *Developments in Block Copolymer Science and Technology*; Hamley, I. W., Ed.; Wiley: Chichester, 2004. (b) Hadjichristidis, N.; Pispas, S.; Floudas, G. *Block Copolymers: Synthetic Strategies, Physical Properties, and Applications*; Wiley: Hoboken, 2003. For block copolymer thin films see: Fasolka, M. J.; Mayes, A. M. *Annu. Rev. Mater. Res.* **2001**, *31*, 323.
(3) For reviews on poly(ferrocenylsilanes) see: (a) Manners, I. *Macromol. Symp.* **2003**, *196*, 57. (b) Kulbaba, K.; Manners, I. *Macromol. Rapid Commun.* **2001**, *22*, 711. (c) Manners, I. *Chem. Commun.* **1999**, 857.
(4) Lammertink, R. G. H.; Hempenius, M. A.; Chan, V. Z.-H.; Thomas, E. L.; Vancso, G. J. *Chem. Mater.* **2001**, *13*, 429.
(5) (a) Nguyen, M. T.; Diaz, A. F.; Dement'ev, V. V.; Pannell, K. H. *Chem. Mater.* **1993**, *5*, 1389. (b) Rulkens, R.; Lough, A. J.; Manners, I.; Lovelace, S. R.; Grant, C.; Geiger, W. E. *J. Am. Chem. Soc.* **1996**, *118*, 12683. (c) Péter, M.; Lammertink, R. G. H.; Hempenius, M. A.; Vancso, G. J. *Langmuir* **2005**, *21*, 5115.
(6) Hinderling, C.; Keles, Y.; Stöckli, T.; Knapp, H. F.; de los Arcos, T.; Oelhafen, P.; Korczagin, I.; Hempenius, M. A.; Vancso, G. J.; Pugin, R.; Heinzelmann, H. *Adv. Mater.* **2004**, *16*, 876.
(7) Wang, X.; Winnik, M. A.; Manners, I. *Macromolecules* **2005**, *38*, 1928.
(8) Cao, L.; Massey, J. A.; Winnik, M. A.; Manners, I.; Riethmüller, S.; Banhart, F.; Spatz, J. P.; Möller, M. *Adv. Funct. Mater.* **2003**, *13*, 271.
(9) Massey, J.; Power, K. N.; Manners, I.; Winnik, M. A. *J. Am. Chem. Soc.* **1998**, *120*, 9533.
(10) Massey, J. A.; Temple, K.; Cao, L.; Rharbi, Y.; Raez, J.; Winnik, M. A.; Manners, I. *J. Am. Chem. Soc.* **2000**, *122*, 11577.
(11) Raez, J.; Manners, I.; Winnik, M. A. *Langmuir* **2002**, *18*, 7229.
(12) (a) Lammertink, R. G. H.; Hempenius, M. A.; Van den Enk, J. E.; Chan, V. Z.-H.; Thomas, E. L.; Vancso, G. J. *Adv. Mater.* **2000**, *12*, 98. (b) Lammertink, R. G. H.; Hempenius, M. A.; Vancso, G. J. *Langmuir* **2000**, *16*, 6245.
(13) (a) Ni, Y.; Rulkens, R.; Manners, I. *J. Am. Chem. Soc.* **1996**, *118*, 4102. (b) Lammertink, R. G. H.; Hempenius, M. A.; Vancso, G. J.; Shin, K.; Rafailovich, M. H.; Sokolov, J. *Macromolecules* **2001**, *34*, 942.
(14) Price, C. *Pure Appl. Chem.* **1983**, *55*, 1563.
(15) Mandema, W.; Zeldenrust, H.; Emeis, C. A. *Macromol. Chem.* **1979**, *180*, 1521.
(16) Canham, P. A.; Lally, T. P.; Price, C.; Stubbersfield, R. B. *J. Chem. Soc., Faraday Trans. 1* **1980**, *76*, 1857.
(17) (a) Zhou, Z.; Chu, B. *Macromolecules* **1988**, *21*, 2548. (b) Schillén, K.; Brown, W.; Johnsen, R. M. *Macromolecules* **1994**, *27*, 4825. (c) Lehner, D.; Lindner, H.; Glatter, O. *Langmuir* **2000**, *16*, 1689.
(18) (a) Zhang, L.; Eisenberg, A. *Science* **1995**, *268*, 1728. (b) Zhang, L.; Eisenberg, A. *J. Am. Chem. Soc.* **1996**, *118*, 3168.
(19) Spatz, J. P.; Mössmer, S.; Möller, M. *Angew. Chem., Int. Ed. Engl.* **1996**, *35*, 1510.

(20) Mortensen, K.; Brown, W.; Almdal, K.; Alami, E.; Jada, A. *Langmuir* **1997**, *13*, 3635.
(21) Tao, J.; Stewart, S.; Liu, G.; Yang, M. *Macromolecules* **1997**, *30*, 2738.
(22) Krupers, M. J.; Sheiko, S. S.; Möller, M. *Polym. Bull. (Berlin)* **1998**, *40*, 211.
(23) (a) Antonietti, M.; Heinz, S.; Schmidt, M.; Rosenauer, C. *Macromolecules* **1994**, *27*, 3276. (b) Zhang, L.; Eisenberg, A. *J. Am. Chem. Soc.* **1996**, *118*, 3168. (c) Discher, D. E.; Eisenberg, A. *Science* **2002**, *297*, 967. (d) Ben-Shaul, A.; May, S. *J. Phys. Chem. B* **2001**, *105*, 630.
(24) Korczagin, I. Poly(ferrocenylsilanes) in Micro- and Nanofabrication: Materials Chemistry and Surface Patterning for Lithography and Catalysis. Thesis, University of Twente, Feb 10, 2005.
(25) Kloninger, C.; Knecht, D.; Rehahn, M. *Polymer* **2004**, *45*, 8323.
(26) Koppel, D. E. *J. Chem. Phys.* **1972**, *57*, 4814.
(27) Frederik, P. M.; Hubert, D. H. W. Cryoelectron Microscopy of Liposomes. In *Methods in Enzymology*; Düzgünes, N., Ed.; Elsevier: Amsterdam, 2005; Vol. 391, p 431.
(28) (a) Spěváček, J. *Makromol. Chem., Rapid Commun.* **1982**, *3*, 697. (b) Godward, J.; Heatley, F.; Price, C. *J. Chem. Soc., Faraday Trans.* **1993**, *89*, 3471.
(29) Candau, F.; Heatley, F.; Price, C.; Stubbersfield, R. B. *Eur. Polym. J.* **1984**, *20*, 685.
(30) Eitouni, H. B.; Balsara, N. P.; Hahn, H.; Pople, J. A.; Hempenius, M. A. *Macromolecules* **2002**, *35*, 7765.
(31) Zero, K.; Pecora, R. Dynamic Depolarized Light Scattering. In *Dynamic Light Scattering, Applications of Photon Correlation Spectroscopy*; Pecora, R., Ed.; Plenum Press: New York, 1985; pp 59−83.
(32) (a) Schurr, J. M.; Schmitz, K. S. *Biopolymers* **1973**, *12*, 1021. (b) Castanho, M. A. R. B.; Brown, W.; Prieto, M. J. E. *Biophys. J.* **1992**, *63*, 1455. (c) Hoffmann, A.; Koch, T.; Stühn, B. *Macromolecules* **1993**, *26*, 7288. (d) Jian, T.; Anastasiadis, S. H.; Fytas, G.; Adachi, K.; Kotaka, T. *Macromolecules* **1993**, *26*, 4706. (e) References 17b and 17c.
(33) Frisken, B. J. *Appl. Opt.* **2001**, *40*, 4087.
(34) Broersma, S. *J. Chem. Phys.* **1960**, *32*, 1626.
(35) 2.5 μm < L_3 < 4.5 μm and 2.4 μm < L_2 < 3.3 μm.
(36) Kim, S. H.; Misner, M. J.; Xu, T.; Kimura, M.; Russell, T. P. *Adv. Mater.* **2004**, *16*, 226.
(37) Lammertink, R. G. H.; Hempenius, M. A.; Manners, I.; Vancso, G. J. *Macromolecules* **1998**, *31*, 795.

MA052521I